

An Automated Potentiometric System For Precision Measurement Of the Quantized Hall Resistance

Volume 92

Number 5

September-October 1987

Giancarlo Marullo Reedtz

Istituto Elettrotecnico Nazionale
Galileo Ferraris,
Strada delle Cacce 91
10135 Torino, Italy

Marvin E. Cage

National Bureau of Standards
Gaithersburg, MD 20899

This paper describes the development of an automated potentiometric measurement system that is used to compare the quantized Hall resistance with that of wire-wound reference resistors having the same nominal value. Conceptual considerations, along with the major practical problems associated with this method, are presented. We then report experimental results which demonstrate that this

measurement system is accurate to within a 0.007 ppm one standard deviation uncertainty.

Key words: electrical metrology; ohm; precision measurements; quantized Hall resistance; quantum Hall effect; resistance standards.

Accepted: March 27, 1987

1. Introduction

The quantization of the Hall resistance

$$R_H(i) = \frac{h}{e^2 i} \approx \frac{25,812.80}{i} \Omega, \quad (1)$$

(where h is the Planck constant, e the electron charge, and i an integer quantum number) has been demonstrated for such diverse two-dimensional electron systems as those in Si-MOSFETs [1]¹ or in heterostructure devices (GaAs/AlGaAs [2] and more recently InGaAs/InP [3]). This resistance quantization provides a very promising means to

yield not only a constant and reproducible as-maintained unit of resistance but to determine also, by solid state physics techniques, the fine structure constant α [4,5]. Even if the physical phenomenon (as manifested in real samples) is not completely understood, the experimental results from different national laboratories show an agreement between R_H values of a few parts in 10^7 [6] when using different samples and measurement systems.

The precision measurement of R_H requires three main steps: 1. the metrological characterization of the sample so that a reasonable confidence is reached on the independence of the measured value from the experimental conditions—mainly temperature and current through the sample [7,8]; 2. the comparison of R_H with the resistance R_R of a highly stable reference resistor; and 3. the calibration of R_R in terms of either the as-maintained unit of resistance or in terms of the International System (SI) resistance unit.

About the Authors: Giancarlo Marullo Reedtz is a physicist at the Galileo Ferraris National Electro-technical Institute, and Marvin E. Cage, who is with the Electricity Division in the NBS Center for Basic Standards, is also a physicist.

¹Figures in brackets indicate literature references.

An automated potentiometric system has been built to compare, as in step 2, the value of R_H with a nominally equal reference resistance R_R within a one standard deviation (1σ) uncertainty of 0.007 ppm (parts per million). This system, which replaces and improves an earlier manually-operated version, is flexible enough to be used also for the precision measurements required in step 1.

2. Comparison of R_H and R_R

The conceptual scheme of the measurement circuit is shown in figure 1, where the numerical values are specific to the case when $R_H=6,453.20 \Omega$ (the $i=4$ Hall plateau) and the current is $I=25 \mu\text{A}$. The two resistances to be compared are connected in series, and the high impedance nanovoltmeter D measures the differences between each voltage drop V_H or V_R and the compensation voltage V_C . The switch S_1 enables the current direction and the compensation voltage both to be reversed so that the influence of thermal-electric voltages can be reduced; S_2 allows for switching between V_H and V_R . Therefore, S_1 must not change the resistance of the current circuits too much for the two polarities,

and S_2 must introduce only a minimum amount of thermal voltages in the voltage circuit.

The measurement sequence needed for a single determination of the ratio R_H/R_R should be chosen to reduce the influence of the thermal voltages and the voltage and current drifts, while also trying to minimize the number of switching operations. Using the letters H or R to represent the comparisons between V_H or V_R and V_C (switch S_2), and the symbols $+$ and $-$ for the two current polarities (switch S_1), we consider the following sequence of operations:

$$R^+, R^-, H^-, H^+, H^-, R^-, R^+. \quad (2)$$

Within each pair of $+/-$ measurements, the influence of the thermals, if constant, is eliminated by the current reversal. The circuit in figure 1 is also affected by changes in the thermals, and by drifts in the voltage generators E and E' , or in the currents. Linear drifts in the circuit can be represented as changing currents by the relations

$$\begin{aligned} I(t) &= I(0)(1 + \beta t) \\ I'(t) &= I'(0)(1 + \beta' t). \end{aligned} \quad (3)$$

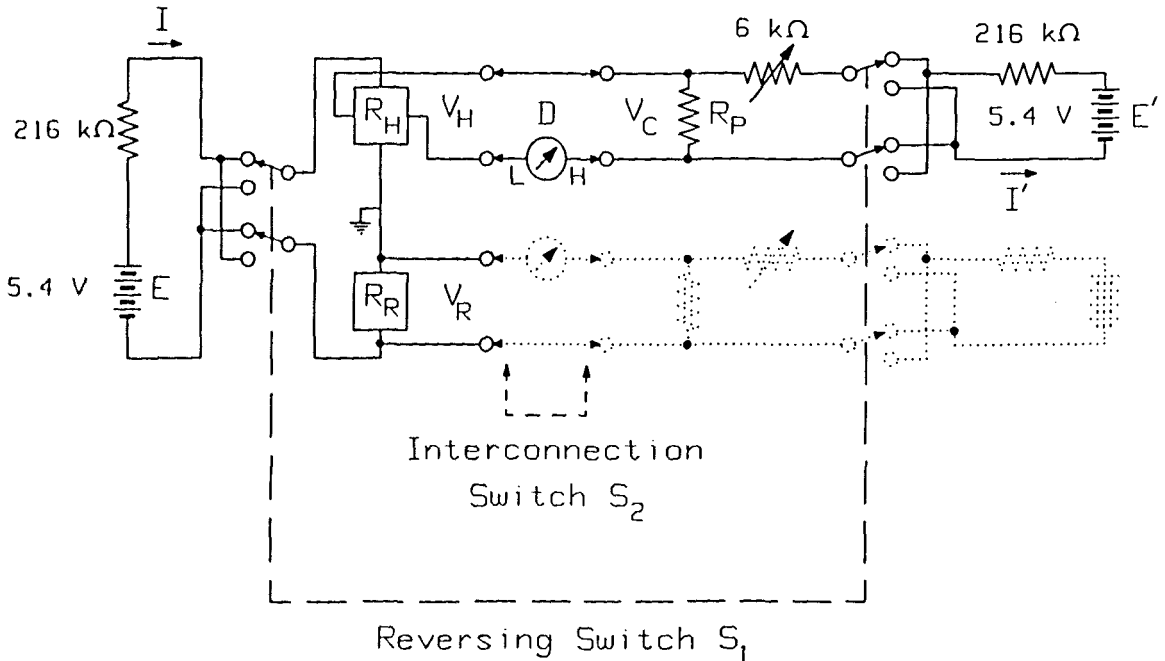


Figure 1-Schematic diagram of the automated potentiometric measurement system which compares the quantized Hall resistance R_H with a nominally equal reference resistor. The voltage sources E and E' are thermally insulated mercury batteries. D is a Leeds & Northrup 9829 Linear Amplifier.

Neglecting constant thermals, we consider a sequence of four measurements R, H, H, R where the following relationships hold:

$$\begin{aligned} I(t_1) \cdot R_R &= I'(t_1) \cdot R_P - D(t_1) \\ I(t_2) \cdot R_H &= I'(t_2) \cdot R_P + D(t_2) \\ I(t_3) \cdot R_H &= I'(t_3) \cdot R_P + D(t_3) \\ I(t_4) \cdot R_R &= I'(t_4) \cdot R_P - D(t_4) \end{aligned} \quad (4)$$

where $D(t)$ is the reading of the detector at time t , and R_P is the potentiometer resistance as labeled in figure 1. If the measurements are uniformly spaced with time intervals Δt , then using eqs (3) and (4) and dividing the sum of the R_H equations by the sum of the R_R equations, we obtain

$$\frac{R_H}{R_R} = \frac{1 + \frac{D(t_2) + D(t_3)}{2V_C(t)}}{1 - \frac{D(t_1) + D(t_4)}{2V_C(t)}} \quad (5)$$

where

$$V_C(\bar{t}) = R_P \cdot I'(0) (1 + \beta' \bar{t}) \quad (6)$$

and $\bar{t} = t_1 + \frac{3}{2}\Delta t$ is the mean time of the four measurements.

If the two resistance values are different by a small amount we can expand the denominator in eq (5); neglecting second-order terms:

$$\frac{R_H}{R_R} \approx 1 + \frac{1}{V_C} \left[\frac{D(t_1) + D(t_4)}{2} + \frac{D(t_2) + D(t_3)}{2} \right] \quad (7)$$

Here the compensation voltage V_C has been written as time independent, which it is in the limits that we require (e.g., V_C need only be constant to 1 part in 10^3 for D/V_C ratios of 10^{-5} if we want an accuracy of 1 part in 10^8). Within these limits the drift of V_C has no influence in eq (7).

We now examine what happens if the switch S_1 introduces slightly different resistances for the two polarities of the I and I' circuits. Let the currents for the two polarities be I and $(-I' + \Delta I')$ for the circuit E , and in a similar way I' and $(-I' + \Delta I')$ for the voltage compensation circuit E' . Consider two successive pairs of measurements R^+, R^- and H^-, H^+ . We can write the relations for the respective detector voltages:

$$\begin{aligned} D_R^+ &= I' \cdot R_P - I \cdot R_R \\ D_R^- &= (-I' + \Delta I') \cdot R_P - (-I + \Delta I) \cdot R_R \\ D_H^- &= -(-I' + \Delta I') \cdot R_P + (-I + \Delta I) \cdot R_H \\ D_H^+ &= -I' \cdot R_P + I \cdot R_H \end{aligned} \quad (8)$$

Subtracting and dividing each pair by two:

$$\begin{aligned} D_R^* &= \frac{D_R^+ - D_R^-}{2} = I' \cdot R_P - I \cdot R_R - \frac{\Delta I' \cdot R_P}{2} + \frac{\Delta I \cdot R_R}{2} \\ D_H^* &= \frac{D_H^+ - D_H^-}{2} = -I' \cdot R_P + I \cdot R_H + \frac{\Delta I' \cdot R_P}{2} - \frac{\Delta I \cdot R_H}{2} \end{aligned} \quad (9)$$

Adding and reordering:

$$\frac{R_H}{R_R} = 1 + \frac{D_R^* + D_H^*}{I \cdot R_R} - \frac{\Delta I}{2I} \left[1 - \frac{R_H}{R_R} \right] \quad (10)$$

The last (third) term in eq (10) gives a second-order correction if the two resistances to be compared are nearly equal and the variation $\Delta I/I$ is small enough. As before, the denominator of the second term need only be known with limited accuracy and can be replaced by the compensation voltage V_C .

As a conclusion of this analysis we note that: a) the sequence given by eq (2) eliminates the effects of constant thermals within each pair of current reversal measurements; b) the symmetrical sequence eliminates the effects of linear drifts of thermals and of I and I' ; and c) the measurements are not influenced by the slightly different values of I and I' for the two current polarities because each polarity is used to compare both V_H and V_R with the same compensation voltage V_C .

The measurement sequence actually used is a little more complex but fulfills all the requirements outlined above. It can be represented by

$$\begin{aligned} R^+, R^-, R^-, R^+, H^+, H^-, H^-, H^+, \\ H^+, H^-, H^-, H^+, R^+, R^-, R^-, R^+ \end{aligned} \quad (11)$$

This sequence provides a single value of the ratio R_H/R_R . If we call the mean values for each group of four measurements D_1, D_2, D_3 , and D_4 , and if we define

$$\begin{aligned} D_R &= \frac{D_1 + D_4}{2} \\ D_H &= \frac{D_2 + D_3}{2} \end{aligned} \quad (12)$$

then the relationship for the R_H/R_R value is

$$\frac{R_H}{R_R} = 1 + \frac{D_H}{V_C} + \frac{D_R}{V_C} \quad (13)$$

3. Sample Characterization and System Flexibility

Every prospective sample must be characterized to establish what experimental conditions are required in order to ensure that the measured values of R_H have the desired accuracy [7,8]. The following measurements of R_H and of R_X (the sample resistance in the direction of the current) are made before a device is considered for precision R_H/R_R comparisons: 1) R_H and R_X as a function of the sample temperature; 2) R_H and R_X as a function of the current through the sample; 3) as in items 1) and 2), but for different pairs of R_H and R_X contacts and for both magnetic field directions; and 4) R_H values for different points along the Hall plateau to verify its flatness.

All these measurements require precision comparisons between R_H and R_R . For item 2) the compensation voltage for R_H measurements must be varied over a wide range. Also, a high impedance current source is required to maintain constant current when the sample is not in a well-quantized regime. The potentiometric comparison circuit of figure 1 has been built in modular form to allow for these different measurement conditions. A functional diagram of the components of this circuit is shown in figure 2, where solid (dashed) lines are for current (voltage) connections. Dashed lines also symbolize output signals that are measured or recorded.

The Potentiometer Box in figure 2 provides the functions needed for the highest precision measurements. The currents I and I' are generated using matched sets of thermally insulated mercury batteries and fixed-value resistors. Comparisons of R_H/R_R can be made at $10 \mu\text{A}$ and $25 \mu\text{A}$ for $i=4$ Hall steps and at $25 \mu\text{A}$ for $i=2$ steps. These currents are small enough to provide accuracies better than 1 part in 10^8 for the three GaAs samples so far characterized.

An electronic, high impedance, constant current source can replace the mercury battery source I of the Potentiometer Box for current dependence measurements and for measurements off of the step. The electrical noise, however, is an order of magnitude higher with the constant current source. A high stability solid-state Zener voltage source

followed by a Kelvin-Varley resistance divider can substitute for the battery current source and fixed divider. These again are an order of magnitude noisier.

The Sample Patch Box allows for easy connection of the current leads to the source and drain, as well as to any pair of potential pads on the sample, e.g., V_H or V_X . The voltages read by the detector can either be direct or compensated by V_C .

Each Reference Resistor Box contains an Electro Scientific Industries resistor², composed of series/parallel combinations of wire-wound resistors constructed to have R_R values within a few ppm of the value of R_H . They are hermetically sealed in a silicone fluid-filled container and placed in a specially constructed temperature-regulated air bath enclosure. The air temperature is controlled to within $\pm 0.002^\circ\text{C}$ at a nominal temperature of $\sim 28^\circ\text{C}$.

The Calibration Box contains an adjustable voltage source whose polarity can be reversed by the Hewlett Packard 9836 computer. This box, when connected to the detector input, enables the detector-digital voltmeter combination to be calibrated.

Finally, R_H and R_R can be easily interchanged in the measurement circuit to check for systematic errors. We have found this test to be essential.

4. Construction Considerations

4.1 The Insulation Resistance

The high values of the resistances to be compared ($6,453.20 \Omega$ or $12,906.40 \Omega$ for $i=4$ or $i=2$ steps, respectively) require an insulation resistance of the circuit of about $10^{12} \Omega$ to achieve an uncertainty of the order of 10^{-8} . As a rule, polytetrafluoroethylene (PTFE or Teflon) has been used as the insulating material. Great care was taken in cleaning the insulating parts of cables and connectors with alcohol. This provides leakage resistances greater than $10^{14} \Omega$.

The switching is done by Leeds & Northrup 4 pole, 12 position, rotary switches with Lexan wafers (model number 031264). The leakage resistance is $5 \times 10^{13} \Omega$ for each connection. Multiple connections reduce this value. The nanovoltmeter detector D is a Leeds & Northrup 9829 Linear Amplifier. Its input low is only isolated by $10^{10} \Omega$ from

²Brand names are used only for purposes of identification. Such use implies neither endorsement by the National Bureau of Standards nor assurance that the equipment is the best available.

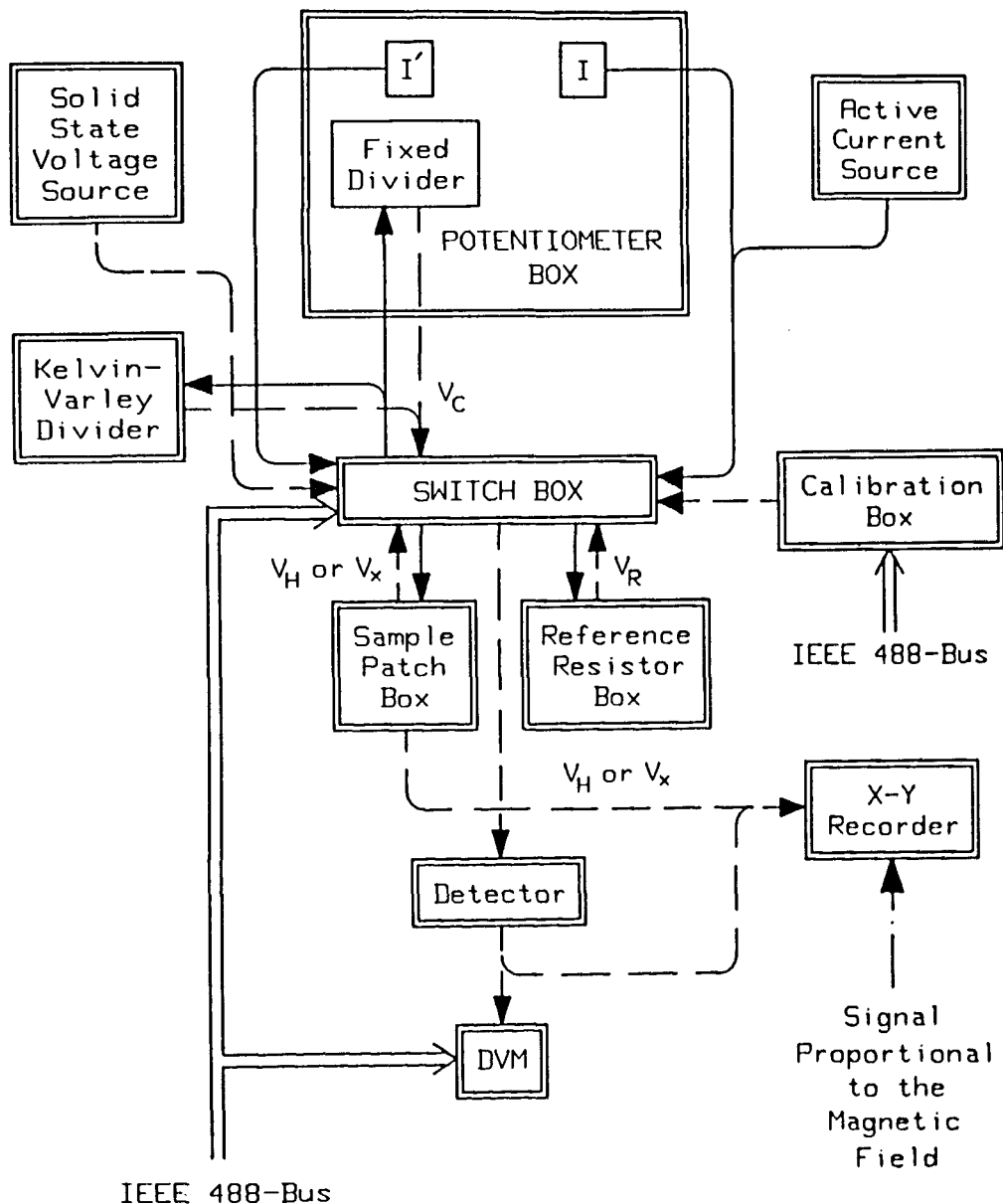


Figure 2—Functional block diagram of the measurement system. This figure stresses the interchangeability of different components to enable the highest precision measurements as well as the physical characterization of the Hall sample. Solid lines represent the current-related functions and dashed lines the voltage-related functions. (There are, of course, actually two paths for every line drawn in the figure.) See the text for further explanation.

the nanovoltmeter guard circuit. Therefore, the detector input low is always connected to the potential point nearest circuit ground, and the guard is also connected to this ground. (The low potential point, of course, changes sides on the sample if the magnetic field direction is reversed.)

The complete potentiometric measurement system has an insulation resistance of $3 \times 10^{12} \Omega$ when the humidity is less than 50%. This leakage resis-

tance is periodically monitored to ensure that dust, lint, hair, and fingerprints have not reduced it.

4.2 Contact Resistances, Thermal-Electric Voltages, and Drifts

The cables consist of sets of twisted pairs of PTFE-insulated, silvered, stranded copper wires enclosed within two separate coaxial shields.

British Post Office connectors (model numbers OFF 66148 and 66149) are used whenever possible because they have small and reproducible contact resistances, high leakage resistances, and are completely shielded.

Fixed connections are made by a low melting point Sn-Pb alloy solder, rather than a low thermoelectric power Sn-Cd alloy, because of better mechanical strength and more reliable electrical contacts. Tightly-packed thermal insulation is used to minimize temperature gradients.

The contact resistances of the Leeds & Northrup rotary switches are less than 0.7 m Ω and have a reproducibility of 0.05 m Ω . Differences in resistance of the two current circuits, due to slightly different lengths of the wires through the switches for each polarity, are less than 4 m Ω . That value is less than 2×10^{-8} of the resistance of each circuit. As shown in section 2, this has no detectable influence on the result when using the sequence of measurements shown in expression (11). These switches exhibit less than 20 nV thermals 10 seconds after repeated switching.

The drifts of the I and I' sources are of the order of 0.2 ppm or less during the 12 minute time intervals required to carry out the measurement sequence of expression (11). This small drift rate is achieved by using careful thermal insulation of the Potentiometer Box, and by not opening the loads during current reversals. (Momentary double loads in the make-before-break switching are better than open-circuiting for the stability of the mercury batteries.)

4.3 The Automated Switching

Stepping motors have been used to rotate the switches S_1 and S_2 . They are Clifton Precision model 23-SHAB-49BU motors with a minimum rotation of 0.9°/step and a 0.45 N·m torque. The motors must overcome a significant frictional force. As a result, they occasionally can miss steps. After several misses the switches may open-circuit. To prevent this we realign the switches by deliberately forcing the motors to rotate the switches against stops.

The motors are controlled by a driver (a Clifton Precision model DPB05) which supplies the clock pulses that control the steps, and other TTL signals which determine the direction of rotation, the working mode (0.9°/step or 1.8°/step), and the current-off-after-switching capability. The last feature is useful to reduce the noise in the system during measurements and to allow for manual switch operation.

4.4 Noise Problems

Great care has been used in shielding the system. Two independent levels of electrostatic shielding have been provided for all the boxes and cables within the instrument. In addition, the electronics rack for the instrument, aluminum shelves for the reference resistors, metal room walls, and copper pipe for the signal cable to the cryostat give a third, nearly complete, shielding level that is electrically insulated from the other two shields. The only exceptions are: the reference resistor boxes which have only two levels of shielding, and the cryostat and quantum Hall sample holder with just one independent shield.

To avoid current loops, all cables have their coaxial shields broken on one side. Shielding connections among different chassis boxes are made by dedicated cables. Only one connection exists between different shielding levels, between the instrument rack and laboratory ground, and between the first shield and the measurement circuit. This last connection can be opened for the leakage resistance tests.

The largest amount of electrical noise in the system comes from the nanovoltmeter detector, which has 150 nV peak-to-peak noise within a 0.5 Hz bandwidth. This noise (obtained with the input short-circuited and with the instrument powered by batteries) corresponds to about 38 nV at the 1σ level, to be compared with 7 nV (1σ) Johnson noise of a 6,453.20 Ω resistor at room temperature within the same bandwidth.

The nanovolt amplifier noise is about 25×10^{-8} of the voltage to be compared for a current of 25 μ A on the $i=4$ step. Therefore, long integration times must be used on the detector output to obtain uncertainties less than 1×10^{-8} for the standard deviation of the mean of a R_H/R_R comparison.

For each operation of the sequence given in expression (11), the computer takes 60 readings in 30 s time intervals from a digital voltmeter at the output of the detector. A wait time of 15 s is introduced after switching. It takes 12 minutes to complete one sequence and thus yield a single value of the ratio R_H/R_R . The standard deviation³ of such a sequence is typically 0.016 ppm. The value is the same whether the reference resistor is compared with a quantum Hall resistor or with another reference resistor. Seven sequences (84 minutes of measurements) are usually sufficient to obtain a standard deviation of the mean (random uncertainty) of 0.006 ppm.

³Throughout, all uncertainties are meant to correspond to one standard deviation estimates.

5. System Performance

This measurement system has been in operation since August, 1986 to compare the value of R_H for the $i=4$ plateau of a GaAs/AlGaAs heterostructure with that of two nominally equal 6,453.20 Ω reference resistors, and to also intercompare the two reference resistors. Table 1 summarizes the estimated uncertainties assigned to quantum Hall sample-reference resistor intercomparisons for a 25 μA current.

Table 1. Estimated one standard deviation (68% confidence level) uncertainties for the quantum Hall resistance measurements at 25 μA .

$R_H \leftrightarrow R_R$	
Sources of Uncertainty	Uncertainty (ppm)
Random	0.004
Sample-Resistor Interchange	0.004
Detector Gain Stability	0.003
Leakage Resistance	0.002
QHR Temperature Dependence	0.002
QHR Current Dependence	<u>0.001</u>
ROOT-SUM-SQUARE TOTAL (ppm)	0.007

The standard deviation of the mean (the random or type A measurement uncertainty) is, as noted above, typically ± 0.006 ppm for a sample-resistor comparison. The position of the sample and resistor are then interchanged in the measurement system and the values are remeasured. The Hall resistance value assigned is the unweighted mean of these two comparisons, and the random uncertainty of the 14 pooled measurements is usually ± 0.004 ppm. Pooling all of the measurements is viewed as justified since usually the difference in the values obtained in the two positions is well within the scatter of the data.

In addition to the random uncertainties, there are systematic, or type B, uncertainties associated with systematic corrections and other effects. One such correction is due to a measurement system offset, or interchange, error in which the value of the Hall resistance depends on whether it is measured in the R_H position or in the R_R position of the measurement circuit. The largest interchange correction to date has been $+0.013$ ppm, but, as noted above, is usually much less (i.e., indiscernible; the correction is based on the assumption that the mean of the two values obtained is the correct value). It is not completely understood why the interchange correction is less of a problem in this measurement system than it is in the old version of the potentiometric

system [9] and in the automated bridge system [9,10]. Perhaps it is due to a higher leakage resistance and to better electrical shielding. The estimated type B uncertainty associated with the interchange correction is assumed to be the same as the random uncertainty: ± 0.004 ppm.

There is an uncertainty in calibrating the gain of the electronic detector-digital voltmeter pair. The pair can appear to vary by a few tenths of a percent over the input voltage range if the DVM has a dead-band at zero volts [9]. The dead-band of our Hewlett Packard 3457A Digital Multimeter is small enough for this effect to be negligible. There remains, however, the problem of the stability of the detector-digital voltmeter gain. The day-to-day gain varies by $\sim 0.1\%$ when the room temperature is controlled to ± 1 $^\circ\text{C}$. This instability contributes an estimated ± 0.003 ppm type B uncertainty to the sample-resistor measurements because our reference resistors are about 2–3 ppm smaller than the quantum Hall resistance.

The 3×10^{12} Ω measurement system leakage resistance contributes an estimated ± 0.002 ppm type B uncertainty.

No temperature-dependent [7] or current-dependent [8] quantized Hall resistance (QHR) corrections could be detected for the Hall-probe set used on this sample. The respective estimated type B uncertainties for the dependence of the QHR on temperature and current are ± 0.002 ppm and ± 0.001 ppm.

The total root-sum-square uncertainty is typically ± 0.007 ppm. This uncertainty is only one third that of the old potentiometric measurement system [9] and the bridge system [9,10]. The smaller uncertainty owes to: a) the ability to directly interchange the sample and the reference resistor positions in the measurement system, rather than having to substitute another reference resistor for the sample in order to determine the interchange error; b) a smaller interchange error; c) the fact that there is only one uncorrelated uncertainty of the detector-digital voltmeter gain, rather than the three correlated uncertainties in the bridge system; and d) a larger leakage resistance.

6. Results

The United States legal unit of resistance Ω_{NBS} is being monitored via the quantum Hall effect [9], as outlined in steps 1 to 3 of section 1. Comparisons between R_H and R_R are made as part of this ongoing procedure. Figure 3 displays the current results. The value of the 6,453.20 Ω reference resistor

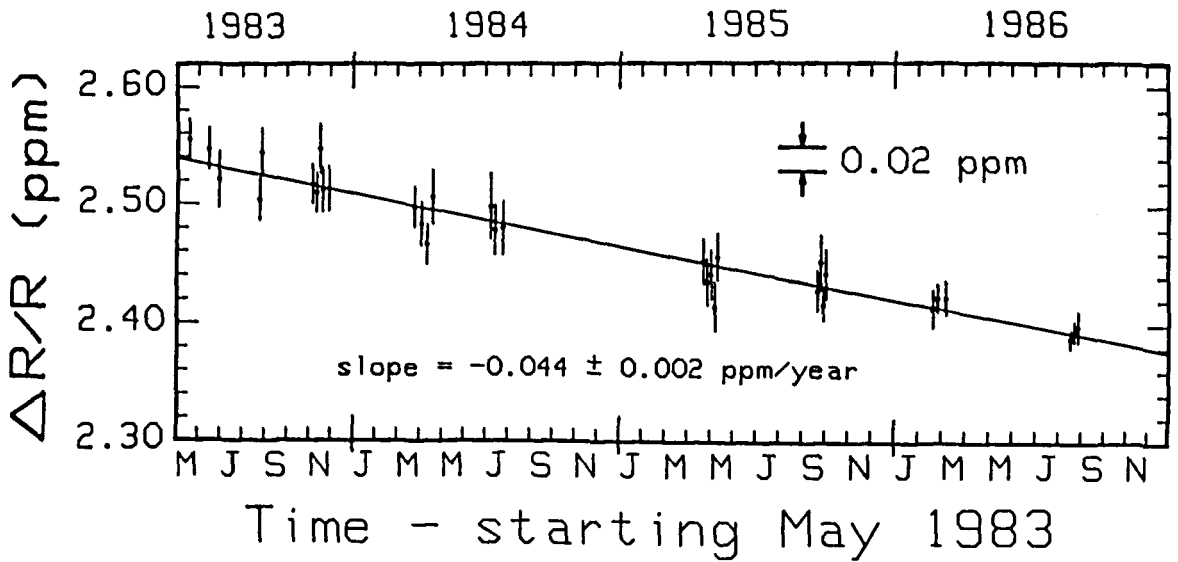
MONITORING A 6453.2 Ω RESISTOR

Figure 3—Relative comparisons as a function of time of the resistance of the $i=4$ steps of three different quantum Hall devices with that of a nominal 6,453.20 Ω wire-wound reference resistor. $\Delta R/R = (V_H - V_R)/V_R$. The value of this resistor is increasing by (0.044 ± 0.002) ppm/year. The last set of data points were obtained with the new measurement system.

used in the comparisons is increasing by (0.044 ± 0.002) ppm/year). The August 1986 data shows the improved measurement accuracy of the new automated potentiometric system over that of the old, manually-operated potentiometric measurement system and the automated bridge system. This new measurement system has proved to be quite reliable, very flexible, and easy to use.

The authors acknowledge having had useful discussions with, and receiving helpful suggestions from, C. T. Van Degrift, T. E. Kiess, B. F. Field, and R. F. Dziuba of the Electricity Division of NBS. One of the authors (G. M. R.) is especially grateful to B. N. Taylor for the opportunity to work on the quantum Hall effect in the NBS Electricity Division.

References

- [1] v. Klitzing, K.; G. Dorda and M. Pepper, New method for high accuracy determination of the fine-structure constant based on quantized Hall resistance, *Phys. Rev. Lett.* **45** 494 (1980).
- [2] Tsui, D. C., and A. C. Gossard, Resistance standard using quantization of the Hall resistance of GaAs/AlGaAs heterostructures, *Appl. Phys. Lett.* **38** 550 (1981).
- [3] Delahaye, F.; D. Dominguez, F. Alexandre, J. P. Andre, J. P. Hirtz, and M. Razeghi, Precise quantized Hall resistance measurements in GaAs/Al_xGa_{1-x}As and In_xGa_{1-x}As/InP heterostructures, *Metrologia* **22** 103 (1986).
- [4] v. Klitzing, K., and G. Ebert, Application of the quantum Hall effect in metrology, *Metrologia* **21** 11 (1985).
- [5] Taylor, B. N., Impact of quantized Hall resistance on SI electrical units and fundamental constants, *Metrologia* **21** 3 (1985).
- [6] For an up-to-date collection of the measurement results from different laboratories see the Proceedings of the Conference on Precision Electromagnetic Measurements 1986, to be published in *IEEE Trans. Instrum. Meas.* **IM-36** (June 1987).
- [7] Cage, M. E.; B. F. Field, R. F. Dziuba, S. M. Girvin, A. C. Gossard, and D. C. Tsui, Temperature dependence of the quantum Hall resistance, *Phys. Rev. B* **30** 2286 (1984).
- [8] Cage, M. E.; R. F. Dziuba, B. F. Field, E. R. Williams, S. M. Girvin, A. C. Gossard, D. C. Tsui, and R. J. Wagner, Dissipation and dynamic nonlinear behavior in the quantum Hall regime, *Phys. Rev. Lett.* **51** 1374 (1983).
- [9] Cage, M. E.; R. F. Dziuba, B. F. Field, T. E. Kiess, and C. T. Van Degrift, Monitoring the U.S. legal unit of resistance via the quantum Hall effect, *IEEE Trans. Instrum. Meas.* **IM-36** (June 1987, to be published).
- [10] Field, B. F., A high-accuracy automated resistance bridge for measuring quantum Hall devices, *IEEE Trans. Instrum. Meas.* **IM-34** 2286 (1984).